

Lycium Barbarum Glycopeptide alleviates neuroinflammation in spinal cord injury via modulating docosahexaenoic acid to inhibiting MAPKs/NF- κ B and pyroptosis pathways.

Zhanfeng Jiang

General Hospital of Ningxia Medical University

Zhong Zeng

General Hospital of Ningxia Medical University

He He

General Hospital of Ningxia Medical University

Mei Li

General Hospital of Ningxia Medical University

Yuanxiang Lan

General Hospital of Ningxia Medical University

Jianwen Hui

General Hospital of Ningxia Medical University

Pengfei Bie

General Hospital of Ningxia Medical University

Yanjun Chen

General Hospital of Ningxia Medical University

Qian Han

General Hospital of Ningxia Medical University

Heng Fan

General Hospital of Ningxia Medical University

Hechun Xia (✉ xhechun@nyfy.com.cn)

General Hospital of Ningxia Medical University Department of Neurosurgery

Research Article

Keywords: Lycium Barbarum Glycopeptide, Docosahexaenoic acid, Neuroinflammation, Spinal cord injury

Posted Date: May 25th, 2023

DOI: <https://doi.org/10.21203/rs.3.rs-2876166/v1>

License:  This work is licensed under a Creative Commons Attribution 4.0 International License.

[Read Full License](#)

Version of Record: A version of this preprint was published at Journal of Translational Medicine on October 31st, 2023. See the published version at <https://doi.org/10.1186/s12967-023-04648-9>.

1 Lycium Barbarum Glycopeptide alleviates neuroinflammation in
2 spinal cord injury via modulating docosahexaenoic acid to inhibiting
3 MAPKs/NF-κB and pyroptosis pathways.

4 Zhanfeng Jiang^{a,b,1}, Zhong Zeng^{a,b,1}, He He^{a,b}, Mei Li^{a,b}, Yuanxiang Lan^{a,b}, Jianwei Hui^{a,b}, Pengfen
5 Bie^{a,b}, Yanjun Chen^{a,b}, Hao Liu^a, Heng Fan^{b**}, Hechun Xia^{b,c*}

6 ^a School of Clinical Medicine, Ningxia Medical University, Yinchuan, Ningxia Hui Autonomous Region
7 750004, P.R, China;

8 ^b Ningxia Key Laboratory of Stem Cell and Regenerative Medicine, Institute of Medical Sciences,
9 General Hospital of Ningxia Medical University, Yinchuan, Ningxia, Autonomous Region 750004, China

10 ^c Department of Neurosurgery, General Hospital of Ningxia Medical University, Yinchuan, Ningxia Hui
11 Autonomous Region 750004, P.R, China;

12 **Key words:** Lycium Barbarum Glycopeptide

13 Docosahexaenoic acid

14 Neuroinflammation

15 Spinal cord injury

16 **First Authors:** Zhanfeng Jiang, Zhong Zeng and He He

17 ***Corresponding Author:** Ningxia Hui Autonomous Region 750004, P.R China

18 ****Corresponding Author:** Ningxia Hui Autonomous Region 750004, P.R China

19 **E-mail Address:** xhechun@nyfy.com.cn (Hechun Xia) fangheng@nxmu.edu.cn (Heng Fan)

20 **Postal Address:** General Hospital of Ningxia Medical University, Yinchuan 750004, Ningxia, China;

21 **ABSTRACT**

22 Background: Lycium barbarum polysaccharides (LBP) is an activity ingredient extracted from Lycium
23 barbarum, which has the effect of inhibiting neuroinflammation. Lycium Barbarum Glycopeptide (LbGp) is
24 a glycoprotein with immunological activity that is further purified and isolated from LBP. Previous studies
25 have shown that LbGp can regulate the immune microenvironment, but its specific mechanism of action
26 is still unclear.

27 Aims: In this study, we aim to explore the mechanism of action of LbGp in the treatment of spinal cord
28 injury through metabolomics and molecular experiments.

29 Methods: SD male rats were randomly assigned to three experimental groups, and after establishing
30 the spinal cord hemisection model, LbGp was administered orally, and the spinal cord tissue was sampled
31 on the seventh day after surgery for molecular and metabolomic experiments. In vitro, LbGp was
32 administered to mimic the inflammatory microenvironment by activating microglia, and its mechanism of
33 action in suppressing neuroinflammation was further elaborated by metabolomics and molecular biology
34 techniques such as western blot, q-PCR.

35 Results: Through in vivo and in vitro experiments, it was found that LbGp can improve the inflammatory
36 microenvironment by inhibiting the NF-κB and pyroptosis pathways. Furthermore, it was found that LbGp
37 can induce the secretion of docosahexaenoic acid (DHA) by microglia, and DHA can inhibit
38 neuroinflammation through the MAPKs/NF-κB and pyroptosis pathways.

39 Conclusions: In summary, we believe that LbGp improves the inflammatory microenvironment by
40 regulating the secretion of DHA in microglia, thereby inhibiting the MAPKs/NF-κB and pyroptosis pathways,

41 promoting nerve repair and motor function recovery. This study provides a new direction for the treatment
42 of spinal cord injury and elucidates the potential mechanism of action of LbGp.
43

44 Introduction

45 Spinal cord injury (SCI) is a highly disabling and lethal disease of the central nervous system (CNS)
46 that lacks effective treatment strategies. The incidence of SCI in China has increased in recent years
47 owing to various factors, such as tumors, hemorrhage, inflammation, and trauma [1], there approximately
48 17000 new patients with SCIs reported annually across the United States [2].

49 Microglia are immune cells in the CNS that play a critical role in neuroinflammation, homeostasis, and
50 stress *in vivo* [3]. Cytokine production mediated by overactivated microglia after SCI triggers an extensive
51 inflammatory cascade, with substantial production of inflammatory factors and reactive oxygen species
52 (ROS) exacerbating the secondary injury, chemokines recruiting peripheral immune cells into the injured
53 area, and reactive nitric oxide species, damage-related molecular patterns (DAMP), and inflammatory
54 signals that induce their entry into the tissues surrounding the injured area, thereby contributing to the
55 clearance of pathogens and cellular debris [4-6].

56 Activation of the cytoplasmic inflammasome is a fundamental step in neuroinflammatory processes and
57 a key trigger for neuronal pyroptosis [7]. To date, five receptor proteins have been confirmed to assemble
58 inflammasomes, including the nucleotide-binding oligomerization domain (NOD), leucine-rich repeat
59 (LRR)-containing protein (NLR) family members NLRP1, NLRP3, and NLRP4, as well as proteins absent
60 in melanoma2 (AIM2) and pyrin [8]. SCI reportedly triggers NLRP3 inflammasome activation in spinal cord
61 microglia [9]. The NOD-like receptor protein-3 (NLRP3) inflammasome, assembled from NLRP3, an
62 apoptosis-associated speck-like protein containing a caspase recruitment domain (ASC), endogenous
63 “danger signal” followed by cysteine protease-1, and exogenous infection, is an important cytosolic protein
64 complex [10]. The activation of the NLRP3 inflammasome requires two key steps and an activation step,
65 in which the binding of DAMP and pathogen-associated molecular patterns to pattern recognition
66 receptors activates the toll-like-receptor (TLR)-myeloid differentiation primary response protein MyD88-
67 nuclear factor- κ B (NF- κ B) pathway to induce inflammasome transcription and trigger post-translational
68 modification. The second step is the assembly and activation of the inflammasome, and inflammasome
69 activation can be achieved through three mechanisms: ROS activation by NADPH oxidase,
70 lipopolysaccharide (LPS) and ATP production, lysosomal rupture, and ion channel gating; NADPH
71 oxidase-mediated ROS play a vital role in this process [7, 11-13]. Activated NLRP3 nucleates the
72 pyroptosis-associated apoptotic protein-containing caspase activation and recruitment domain (CARD)
73 helical fibrils to form ASC patches, which recruit and activate pro-caspase-1 cleavage and activation of
74 pro-interleukin (IL)-1 β , pro-IL-18, and GSDMD [11]. Cleavage of the N-terminal end of GSDMD drives
75 pyroptosis, which leads to cell death and allows cells to release mature IL-1 β and IL-18 [8, 14].

76 LbGp is a glycoprotein with immunological activity that is further purified and isolated from LBP [15].
77 Following metabolomic analysis (Ningxia Tianren GoJi Biotechnology, Ningxia, China), we have previously
78 revealed that LbGp comprises 368 metabolites, including 42 others (40%), 118 terpenoids (32%), 38
79 alkaloids (10%), 24 phenylpropanoids (6.5%), 17 phenols (4.6%), 17 flavonoids (4.6%), 4 amino acids
80 (1.1%), 3 aliphatic acyl (0.8%), and 3 fatty acids (0.8%). However, the precise LbGp component that
81 improves the inflammatory microenvironment *in vivo* by inhibiting MAPKs- NF- κ B and pyroptosis-related
82 pathways needs to be identified.

83 In the present study, we aimed to establish that LbGp induces microglia to secrete DHA *in vivo* to

84 promote nerve regeneration and motor function repair and improve the inflammatory microenvironment
85 by inhibiting MAPKs-NF-kB, and pyroptosis-related pathways, providing a new direction for the treatment
86 of SCI. Accordingly, we performed *in vivo* and *in vitro* molecular and metabolite analyses experiments.

87 **2.Methods and materials**

88 **2.1 Animals**

89 In total, 70 (8-weeks old) male Sprague-Dawley rats (300-350 g) were purchased from the Laboratory
90 Animal Center Ningxia Medical University. After surgery, all rats were housed under continuous
91 temperature (21±3°C) and humidity (50%±5%) with a 12-h light/dark cycle. The experimental protocol was
92 approved by the Laboratory Animal Ethical and Welfare Committee of the Laboratory Animal Center of
93 Ningxia Medical University.

94 **2.2 Rats spinal cord injury model and treatments groups**

95 The twelfth thoracic vertebral body (T12) hemisection model was used as previously described [16].
96 To establish the SCI model, rats were anesthetized with isoflurane (2-4% induction, 1.5% maintenance),
97 and body temperature was maintained at 35±1°C using a mini heating pad. The skin of the upper thoracic
98 area was exposed after shaving and cleaning with betadine solution. To expose T12, the fascia and
99 muscle were bluntly dissected to avoid spinal dural injury during the incision of the dorsal lamina. A needle
100 (26G) was bent by 90° to establish a lateral hemisection, and the spinal cord was punctured dorsoventrally
101 at the middle line by inserting the needle 5 mm while averting damage to the dorsal spinal artery. The left
102 half of the spinal cord was pulled and cut, repeated three times to ensure completeness of the spinal cord
103 hemisection (Fig.S2A-B). For pain management, carprofen (4 mg/kg; Rimadyl®, Zoetis, Florham Park,
104 NJ) and buprenorphine (0.2 mg/mL; Temgesic®, Intervet International, Boxmeer, the Netherlands) were
105 administered continuously before surgery and every 8 h for three successive days after SCI.

106 Forty-five adult male rats were randomly assigned to Three groups (15 rats per group): sham group;
107 SCI group; post-SCI LbGp treatment group; LbGp dissolved in 0.01M phosphate buffer saline at room
108 temperature; LbGp administered via a nasogastric tube (50 mg/kg) once daily until day 28 post-SCI. The
109 sham, SCI groups were administered 0.01M phosphate buffer saline 24 h after SCI.

110 **2.3 Behavioral testing**

111 We next evaluated hind limb motor function in rats after SCI. Three rats were selected from each group,
112 and the Basso-Beattie-Bresnahan (BBB) test was used to score the motor function of the hind limbs. The
113 BBB test is divided into 22 grades, with 21 points indicating normal paralysis and 0 points indicating
114 paralysis. The scoring was performed at 8 p.m. using a double-blind method. Each rat was measured
115 three times, and the average value was recorded.

116 **2.4 Western blot**

117 The rat microglia (RM) cell line (BNCC 360237) was purchased from the BeNa culture collection
118 (Henan, China). First, RM cells were seeded in six-well plates (1×10⁵ cells/well) and activated with LPS
119 (1 µg/ml L3129 Sigma) and ATP (5 mM; Sigma) for 4 h, followed by treatment with LbGp or DHA for 24 h
120 to establish the LbGp treatment group or DHA treatment group. In addition, microglia activated with
121 ATP+LPS were incubated with the FADs2 enzyme inhibitor SC26196 for 12 hours and then incubated
122 with LbGp for 24 hours to construct the ATP+LPS+ SC26196+ LbGp treatment group. Spinal cord tissue

123 was harvested on day 7 post-SCI. Tissue or cell lysates were prepared using the Keygen protein extraction
124 kit (KGP250 Keygen BioTECH China), and the protein concentration was measured with the BCA protein
125 assay kit (KGP902 Keygen BioTECH China). Equal amounts of protein were separated with 10 or 15%
126 sodium dodecyl sulfate-polyacrylamide gel, transferred to polyvinylidene fluoride membranes, and
127 blocked with 5% skim milk. Subsequently, the membranes were probed with the following primary
128 antibodies at 4°C overnight: anti-brain-derived neurotrophic factor (BDNF) (1:10000) (Cat. Number:
129 ab108319; Abcam UK), anti-glia-derived neurotrophic factor (GDNF) (1:2000) (Cat. Number: A14639;
130 ABclonal China), anti-P-p-38 (1:1000) (Cat. Number:28796-1-AP; Proteintech, China), anti- p38 (1:1000)
131 (Cat. Number:14064-1-AP; Proteintech, China), anti-P-p-JNK (1:1000) (Cat. Number:80024-1-RR;
132 Proteintech, China), anti- JNK (1:1000) (Cat. Number:24164-1-AP; Proteintech, China), anti-p-P65
133 (1:1000) (Cat. Number: ab76302; Abcam, Cambridge, UK), anti-p65 (1:20000) (Cat. Number: 80979-1-
134 RR; Proteintech, China), anti-NLRP3 (1:2000) (Cat. Number: 27458-1-AP; Proteintech, China), anti-ASC
135 (1:3000) (Cat. Number:10500-1-AP; Proteintech, China), anti-Caspase-1 p45 (1:1000) (Cat. Number:
136 ab179515; Abcam UK), anti-Caspase-1 p20 (1:2000) (Cat. Number: bs-10442R; Bioss, China), anti-
137 GSDMD and anti-GSDMD-N (1:1000) (Cat. Number: ab219800; Abcam, UK), anti-pro-IL-18 and anti-IL-
138 18 (1:10000) (Cat. Number:10663-1-AP; Proteintech, China), anti-IL-1 β (1:1000) (Cat. Number: ab254360;
139 Abcam, UK), anti- β -actin (1:40000) (Cat. Number: 81115-1-RR; Proteintech China). The membrane was
140 washed with TBST and incubated with a secondary antibody (1:20000) (Cat. Number: ab6721 Abcam UK)
141 for 1 h at room temperature, washed again, visualized with ECL reagent (SW134-01 Seven Biotech,
142 China), and quantitatively analyzed using ImageJ software (National Institutes of Health, Bethesda, MD).

143 2.5 Cell viability assay

144 The Cell Counting Kit-8 (CCK-8) assay (Dojindo Laboratories Lot.CK04 Japan) was used to assess
145 the toxicity of LbGp toward microglia. Microglia were plated in 96-well plates at 7×10^3 cells/well, and
146 different concentrations of LbGp were added (100, 200, and 400 μ g/ml), followed by incubation at 37°C
147 in a 5% CO₂ incubator for 24 h. Then, the supernatant was discarded, and 100 μ l of the medium containing
148 10% CCK-8 reagent was added to each well, followed by incubation at 37°C in a 5% CO₂ incubator for 2
149 h in the dark. The absorbance of each well was detected under the 450 nm wavelength spectrum of a
150 microplate reader.

151 2.6 Enzyme-linked immunosorbent assay analysis (ELISA)

152 Level of DHA in each group were detected by COIBO BIO (Shanghai China). RM cells were seeded
153 in six-well plates (1×10^5 cells/well) and activated with LPS (1 μ g/ml L3129 Sigma) and ATP (5 mM; Sigma)
154 for 4 h, followed by treatment with LbGp for 24 h, the cell were centrifuged at 4°C, 800g for 10 min, and
155 200 μ l of supernatant was then collected for DHA detection. DHA assays were performed according to the
156 protocol provided by the COIBO BIO (CB14901-Ra Shanghai China).

157 2.7 RNA preparation and reverse transcription-quantitative PCR

158 Microglia were counted and plated into a six-well plate at a density of 1×10^5 cells/well. On reaching 80%
159 confluency, cells were incubated with 1 μ g/ml LPS for 12 h and then treated with different concentrations
160 of LbGp (100, 200, 400 μ g/ml), followed by incubation for 24 h. After washing three times with cold
161 phosphate-buffered saline (PBS), 1 ml of Trizol was added and pipetted into a 1.5 ml EP tube, followed
162 by 200 μ l of chloroform. The prepared samples were centrifuged at 9000 \times g at 4°C for 15 min. The
163 supernatant was aspirated, and an equal volume of isopropanol was added, followed by centrifugation at

164 9000×g at 4°C for 15 min. The supernatant was removed, and 75% ethanol was added, followed by
165 centrifugation at 6000G×g twice for 5 min at 4°C. The RNA concentration was measured after adding
166 double-distilled water (ddH₂O). The reverse transcription kit and real-time quantitative PCR kit were all
167 purchased from Vazyme (lot. R302-01, Q411-02; Nan Jing, China) and performed according to the
168 manufacturer's instructions. Gene specific primer sequences used are shown in
169 supplementary Table 1. The relative gene expression was measured using the $2^{-\Delta\Delta ct}$ method.

170 2.8 Immunofluorescence staining

171 Rat spinal cord tissue was collected on day 7 post-SCI, which was then subjected to fixation,
172 paraffinization, dewaxing, dehydration, antigen extraction, and blocking, according to the standard
173 protocol. Subsequently, tissue sections were incubated with primary antibodies against anti-NLRP3, anti-
174 ASC, anti-Caspase-1, and anti-NeuN (1:2000) (Cat. Number:6975-1-AP; Proteintech, China) for 24 h.
175 Next, tissue sections were incubated with fluorescent-labeled secondary antibody green (1:500)
176 (ab150077; Abcam UK), red (1:200 SA00013-4; Proteintech, Wuhan, China), rose red (1:200 GB21303
177 Servicebio China), pink (1:200 GB1232 Servicebio China) for 3 h, and the nuclei were stained with DAPI.
178 Images were scanned using an ortho-fluorescent microscope (Nikon eclipse C1) and a fluorescence
179 microscope (Olympus, Japan). Quantitative analysis was performed using ImageJ.

180 2.9 Metabolite processing and identification

181 One-week post-SCI, three groups (A: sham group, B: SCI group, C: LbGp treatment groups; n=six rats/
182 group) were anesthetized under excessive isoflurane, and the dorsal skin surface was incised. The
183 vertebrae were cut, and the injured area of the spinal cord tissue was harvested (approximately 50 mm in
184 length and approximately 30 mg in weight). The harvested spinal tissue was quickly placed in liquid
185 nitrogen and transferred to a -80°C refrigerator for metabolomic sequencing analysis.

186 Metabolomics was performed by Shanghai Luming Biotech Co.Ltd. All reagents were of high-pressure
187 liquid chromatography (HPLC) grade. L-2-chlorophenylalanine was purchased from Shanghai Heng
188 Chuang Bio-technology (Shanghai, China), methoxyamine hydrochloride (97%), pyridine, n-hexane, and
189 BSTFA with 1% TMCS were purchased from CNW Technologies GmbH (Düsseldorf, Germany).
190 Chloroform was obtained from Titan Chemical Reagent (Shanghai, China), and water and methanol were
191 obtained from Thermo Fisher Scientific (Waltham, USA).

192 Briefly, 30 mg of sample was added to a 1.5 ml centrifuge tube, followed by the addition of two small
193 steel beads and 600 µl methanol-water (V:V+4:1, containing L-2-chlorophenylalanine, 4 µg/ml) and
194 incubation for 2 min. The samples were placed in a grinder (60 Hz, 2 min); 120 µl of chloroform was added
195 and vortexed for 2 min. Ultrasonic extraction was performed in an ice-water bath for 10 min at -40°C or
196 for 30 min. Subsequently, centrifugation was performed for 10 min (12000×g 4°C). Next, 150 µl of the
197 supernatant was placed in a glass derivatization bottle, and the sample was dried using a centrifugal
198 concentrator desiccator. Next, 80 µl of methoxyamine hydrochloride pyridine solution (15 mg/ml) was
199 added to the glass derivatized vial, and the sample was vortexed for 2 min and placed in an incubator
200 maintained at 37°C for 60 min to perform the oxidation reaction. After removing the sample, 50 µl of BSTFA
201 derivatization reagent and 20 µl of n-hexane were added, and 10 internal standards
202 (c8/c9/c10/c12/c14/c16/c18/c20/c22/c24, all prepared in chloroform; 10 µl) were added, vortexed for 2
203 min, and reacted at 70°C for 60 min. The obtained samples were placed at room temperature for 30 min
204 to undergo gas chromatography-mass spectrometry (GC-MS) metabolomic analysis. Quality control
205 samples were prepared by mixing equal volumes of extracts from all samples.

206 GC-MS was performed using a Db-5MS capillary column (30×0.25 mm×0.25 μm; Agilent J&W Folsom,
207 CA, USA), high-purity helium (purity ≥ 99.999%) as the carrier gas, a flow rate of 1.0 ml/min, and
208 maintaining an injection port temperature of 260°C. The injection volume was 1 μl, and the injection was
209 split with a solvent delay of 5 min. The program temperatures were as follows: the initial temperature of
210 the column oven was 60°C, maintained for 0.5 min; the program temperature was increased to 125°C at
211 8/min; heated up to 210°C at 8°C/min; 270°C at 15°C/min; 305°C at 20°C/min and maintained for 5 min.

212 For the electron bombardment ion source: ion source temperature, 230°C; quadrupole temperature,
213 150°C; electron energy, 70 eV. The scanning mode was full scan mode (SCAN), with a mass scanning
214 range of 50-500 m/z.

215 The collected GS/MS raw data were converted into abf format by analyzing using Analysis Base File
216 Convert to retrieve data quickly. The data were then imported into the MS-DIAL software for
217 characterization, MS2Dec deconvolution, peak alignment, peak identification, peak detection, wave
218 filtering, and missing value interpolation. Metabolites were characterized based on the LUG database.
219 The data matrix included the signal intensity, retention index, retention time, mass-to-charge ratio, sample
220 information, and peak name for each species. After screening, all peak signal intensities were segmented
221 and normalized for each sample according to an internal criterion of RSD >0.3. After data normalization,
222 redundancy removal and peak merging were performed to obtain a data matrix.

223 The matrix was imported into R for principal component analysis to observe the overall distribution
224 between samples and the stability of the entire analysis process. Different metabolites between groups
225 were distinguished using Orthogonal Partial Least Squares Discriminant analysis (PLS-DA). A 7-fold
226 cross-validation and 200-response permutation test were employed to assess the model quality.

227 The projected importance values of the variables from the OPLS-DA model were used to rank the overall
228 contribution of each variable to the group discrimination. Two-tailed Student's t-test was performed to
229 verify whether the difference in metabolites between groups was significant. Differential metabolites with
230 variable importance of projection value >1.0 and P-value <0.05 were selected.

231 2.10 Statistical analysis

232 Data are presented as mean ± S.D. One-way analysis of variance (ANOVA) was used to assess
233 differences in comparisons of multiple group designs. All statistical analyses were performed using
234 GraphPad Prism (version 9.3). P<0.05 was considered statistically significant.

235 3. Result

236 3.1 LbGp promotes motor function recovery after SCI.

237 LbGp is purified from LBP and contains 368 metabolites (Fig.S1A). LBP is known to repair nerve
238 regeneration and promote motor function recovery [17]. To test our conjecture, by constructing a rat spinal
239 cord hemisection model, oral LbGp was given post-operation, and the motor function of the different
240 treatment groups was assessed up to 28 days after surgery by using the BBB motor function score. Based
241 on the BBB test results, the SCI group score was significantly lower than that of the sham group; the LbGp
242 group score did not significantly differ from that of the SCI group during the first-week post-SCI but was
243 higher than that of the SCI group during the second week (Fig.1A). These results revealed that LbGp
244 treatment could improve motor function in rats. On day 14, the BBB motor function score in the LbGp
245 intervention group was higher than that in the SCI group.

246 3.2 LbGp regulates neurotrophic factors to promote nerve

247 regeneration

248 Previous studies have shown that BDNF and GDNF play an important role in promoting nerve
249 regeneration[18]. To further elucidate the potential role of LbGp on nerve regeneration, we detected the
250 expression levels of BDNF and GDNF in spinal cord injury by western blot and Neun protein by
251 immunofluorescence. Considering that the inflammatory microenvironment was altered prior to behavioral
252 changes in the animals, to further investigate the mechanism of motor function recovery in rats, we
253 examined brain-derived neurotrophic factor (BDNF) and glia-derived neurotrophic factor (GDNF) in the
254 spinal cord tissues of rats on day 7. On day 7, expression levels of BDNF and GDNF proteins were
255 significantly higher in LbGp-treated rat spinal cord tissues than those in the SCI group, as determined by
256 western blotting (Fig.1B-D) (Fig.S3A-B). On day 7, the expression of NeuN protein in spinal cord tissue
257 was consistent with the above results, as determined in tissue immunofluorescence experiments (Fig.1E-
258 F). Therefore, we suggest that LbGp could promote neuronal repair and improve motor function after SCI
259 in rats by modulating BDNF and GDNF.

260

261 3.3 LbGp inhibit NF-kB and pyroptosis-related proteins *in vivo*

262 The role of LbGp in inhibiting neuroinflammation has been demonstrated[19]. To further confirm the role
263 of LbGp in neuroinflammation, we administered different concentrations of LbGp after spinal cord injury
264 by gavage treatment to assess the optimal concentration for its therapeutic effect. The inhibitory effect of
265 different concentrations of LbGp on neuroinflammation was assessed by western blot experiments. Rats
266 were treated with different concentrations (10, 50, and 100 mg/kg) of LbGp after SCI, and the inflammatory
267 factor Pro-IL-18 was detected in the different treatment groups. We observed that LbGp afforded superior
268 inhibition of the inflammatory factor Pro-IL-18 50mg/kg (Fig.2A) (Fig.S3C). Accumulated evidence has
269 shown that LBP can inhibit the expression of the NLRP3 inflammasome and ROS production to suppress
270 inflammation [20]. To further elucidate the mechanism of LbGp's role in spinal cord injury-induced
271 neuroinflammation, we used immunofluorescence and western blot to detect NLRP3, ASC, and Caspase-
272 1 proteins. Compared to SCI group, expression levels of NLRP3, ASC, and Caspase-1 proteins
273 determined by tissue immunofluorescence were significantly reduced in the LbGp group (Fig.2B-D).
274 Based on the western blot analysis, rats in the SCI group exhibited elevated expression of P-p-65, NLRP3,
275 ASC, Caspase-1p45, GSDMD, GSDMD-N, IL-1 β and IL-18 proteins in the spinal cord at day 7 post-SCI;
276 these expression levels were significantly reduced in the LbGp group (Fig.2E-M) (Fig.S3D-E).

277

278 3.4 LbGp inhibit MAPKs/NF-kB and pyroptosis-related proteins *in*

279 *vitro*

280 As mentioned above, LbGp can inhibit the NF-kB and pyroptosis pathways to suppress
281 neuroinflammation *in vivo*, but the target cells on which it acts are unclear. Microglia are intrinsic immune
282 cells in the CNS that are involved in the immune response *in vivo* and play an essential role in
283 neuroinflammation[21]. To determine the effect of LbGp on microglia, a CCK-8 assay was used to examine
284 the cell viabilities. The results indicated that there were no significant changes in cell viabilities when
285 incubation in 100-400ug/ml LbGp (Fig.S4A). To further assess the optimal drug concentration for LbGp
286 inhibition of inflammation triggered by microglia, we incubated LbGp at different concentrations (100,200

287 and 400ug/ml) for 24 h after microglia activation and assayed the expression levels of the inflammatory
288 factor IL-18 mRNA. The RNA of IL-18 was reduced in both LbGp group (100,200 and 400ug/ml), and there
289 was no significant difference between the LbGp groups (Fig.3A). Combining the above results, we gave
290 100ug/ml of LbGp intervention after microglia activation. As previously described, administration of LbGp
291 treatment after activation of microglia resulted in lower expression of P-p38, P-JNK, P-p65, NLRP3, ASC,
292 Caspase-1p20, GSDMD, GSDMD-N, IL-18, and IL-1 β proteins in the LbGp-treated group compared to
293 the ATP+LPS group (Fig.3B-K).

294

295 3.5 LbGp inhibits MAPKs/NF-kB and pyroptosis-related proteins by 296 modulating DHA

297 As described before, LbGp inhibited neuroinflammation both in vivo and in vitro, and to further clarify
298 the mechanism of LbGp treatment for spinal cord injury by metabolomic analysis, 66 metabolites were
299 found to be elevated in cell supernatants and 38 in tissues in the LbGp-treated group (Fig.S5A-E). By
300 matching comparisons, we found that both ethanolamine and docosahexaenoic acid were increased in
301 tissue and cell supernatants after LbGp intervention (Fig.4C). At present, the role of ethanolamine in
302 neuroinflammation is not clear[22-24]. The view that DHA suppresses inflammation by inhibiting the
303 NLRP3 protein in activated macrophages is well confirmed. [25-27]. DHA intervention given after spinal
304 cord injury in rats can inhibit neuroinflammation[28]. Therefore, we reasoned that LbGp may suppress
305 neuroinflammation by regulating DHA production by microglia. To test this view, we administered SC-
306 26196, a inhibitor of FADS2, a key enzyme for DHA production, before LbGp intervention, and the results
307 showed that the effect of LbGp in inhibiting inflammation was significantly weakened after reduced DHA
308 production (Fig.3B-L).

309

310 3.6 LbGp induces DHA secretion from microglia

311 Whether LbGp can induce DHA secretion from microglia, we detected cell supernatants by ELISA and
312 found that DHA was significantly elevated in the LG intervention group (Fig.4D). Metabolomic analysis
313 showed that microglia are rich in DHA, providing the possibility of DHA secretion[29]. FADS1 and FADS2
314 play an essential role in the process of DHA synthesis[30]. Q-PCR results showed that LbGp intervention
315 significantly contributed to high expression of FADS1 and FADS2 mRNA, key enzymes for DHA production
316 (Fig.4E-F).

317

318 3.7 DHA inhibit MAPKs/NF-kB and pyroptosis-related proteins *in*

319 *vitro*

320 Previous study suggest that DHA can inhibit microglia-induced neuroinflammation[31]. Therefore, we
321 further verify its role in the MAPKs/NF-kB and pyroptosis pathway through WB experiments. As previously
322 described, administration of DHA treatment after activation of microglia resulted in lower expression of P-
323 p38, P-JNK, P-p65, NLRP3, ASC, Caspase-1p20, GSDMD, GSDMD-N, IL-18, and IL-1 β proteins in the
324 DHA-treated group (Fig.A-K).

Discussion

In this study we demonstrated for the first time that oral LbGp can improve the SCI inflammatory microenvironment and promote spinal cord repair by inhibiting MAPKs-NF-kB/pyroptosis-related pathways, the exact mechanism of which has not been previously reported.

Spinal cord injury is often accompanied by hemorrhage, peripheral tissue edema, secondary neuroinflammation, and glial scar formation, and these adverse factors severely limit nerve regeneration and functional recovery[32, 33]. There are two stages of spinal cord injury; primary SCI includes spinal cord tissue breakdown, hemorrhage, and destruction of the glia membrane [32]. SCI is a delayed and progressive tissue injury following primary SCI. Ionic homeostasis imbalance in tissues after SCI leads to mitochondrial dysfunction and release of reactive oxygen species, resulting in oxidative stress damage to tissue; damaged cell lead to upregulation of excitatory amino acids and excitotoxicity leading to apoptotic necrosis; inflammatory cells such as microglia and macrophages infiltrate blood-brain-barrier disruption the damaged area and release inflammatory factors [34].

In recent years an increasing number of herbal extracts have been used to study their neuroprotective mechanisms of action. It has been reported that *Gastrodia elata* Blume could increase the cell viability of embryonic neural progenitor cells under hypoxic condition by improving DNA damage repair ability[35]. Danshen extract play a beneficial role in the recovery of locomotor function following SCI in rats. Meanwhile, this effect may be associated with the promotion of axonal regeneration, up-regulation of BDNF, and activation of microglial cells[36]. Iridoid glycosides of *Paederia scandens* possesses antinociceptive effect, which may be partly related to the inhibition of NO/cGMP/PKG signaling pathway in the rat spared nerve injury model of neuropathic pain[37]. Previous research revealed that aloe-emodin protected against brain damage, which is primarily attributed to the antioxidant and anti-neuroinflammatory properties of AE via the PI3K/AKT/mTOR and NF-kB activation[38]. LBP is an activity ingredient extracted from *Lycium barbarum*, which can improve inflammatory microenvironmen [39, 40]. However, the mechanism of action of LBP derivative LbGp in spinal cord injury is unclear.

After spinal cord injury, a large amount of ROS and ATP can activate the release of NLRP3, ASC, Caspase-1, GSDMD and other key proteins related to pyroptosis and related inflammatory factors, which lay a very important role in spinal cord injury[11, 41]. To further verify the mechanism of action of LbGp in inhibiting pyroptosis in spinal cord injury, we found that the LbGp treatment groups could inhibit the expression of key protein p-P38/p-JNK in MAPKs pathways, p-P65 in NF-kB pathway, NLRP3, ASC, caspase-1, GSDMD and downstream inflammatory factors such as IL-18 and IL-1 β in western blot experiments. The specific mechanism of pyroptosis inhibition in the LbGp treatment groups has not been clarified. Herein, levels of unsaturated fatty acid DHA were elevated in the LbGp groups, as determined by assessing the metabolism of microglia and tissues. Previous studies have shown that the unsaturated fatty acid DHA can inhibit NLRP3 and other key proteins of pyroptosis[25]. Unsaturated fatty acids reduce injury-related oxidative stress, decrease microglia/macrophage responses, and improve motor function and bladder function recovery in rats [42]. Following entry into the brain, DHA is esterified into and recycled amongst membrane phospholipids contributing the distribution of DHA in brain phospholipids. During neurotransmission and following brain injury, DHA is released from membrane phospholipids and converted to bioactive mediators which regulate signaling pathways important to synaptogenesis, cell survival, and neuroinflammation, and may be relevant to treating neurological diseases[43]. It has been shown that 3 months of DHA treatment prevents microglia activation after ischemic injury, reduces the

368 size of ischemic lesions, and increases the level of the anti-apoptotic molecule Bcl-2 in the brain[44]. In
369 addition, when we inhibit the DHA-producing pathway in microglia, the effect of LbGp to improve the
370 neuroinflammation is reduced. suggesting that LbGp inhibits SCI pyroptosis by regulating unsaturated
371 fatty acid DHA. Accordingly, LbGp contains diverse metabolites (Fig.S1A); however, which metabolite
372 plays the main role in inducing DHA release from microglia is not clear and needs to be further elaborated
373 in future experiments.

374 LbGp can promote BDNF and GDNF to repair nerve damage. GDNF is a potent promoter of central
375 and peripheral neurons, and BDNF is a major regulator of energy homeostasis that upregulates
376 antioxidant enzymes to enhance repair of damaged neurons, promote differentiation of neurons and stem
377 cells, promote neural protrusion growth and synapse formation, and prevent programmed cell death and
378 apoptosis[18, 45-48]. DHA can promote high BDNF expression [49]. We found that LbGp promoted high
379 expression of BDNF and GDNF in vivo experiments with Western blot further validated this conclusion.
380 The results of immunofluorescence protein NeuN in spinal cord tissue indicated that the LbGp treatment
381 group promoted neuronal repair, and the results of behavioral BBB function score in rats were found that
382 LbGp can improve motor function in rats after spinal cord injury. BBB motor function score suggests that
383 treatment of spinal cord injury in rats with LbGp significantly improves motor function by the second week.
384 Therefore, we hypothesize that LbGp plays a role in the upregulation of BDNF and GDNF through
385 modulate DHA in promoting the recovery of motor function in rats.

386 Conclusion

387 To the best of our knowledge, we, for the first time, report the mechanism of action of LbGp, a
388 polysaccharide derivative of LBP, for treating SCI, which induce microglia secret DHA to inhibit cellular
389 pyroptosis. Because LbGp is widely available at low cost and has an excellent safety profile, which will
390 provide new direction for treating spinal cord injuries

391 Author Contribution

392 Zhanfeng Jiang, Zhong Zeng, He He, Mei Li, Pengfen Bie, Yuanxiang Lan, Jianwen Hui, and Yanjun Chen
393 acquired experiment data, Hao Liu, afford material support, Zhanfeng Jiang drafted the manuscript,
394 Hechun Xia and Heng Fan were involved in study design and supervision.

395 Conflict of interest

396 The authors declare that they have no conflict of interest.

397 Acknowledgements

398 This work was supported by Key technology development of to promote nerve injury repair through
399 modulation of cell microenvironment [grant numbers:2022BEG01004. (Kwok-Fai So, HeChun Xia). At the
400 end of the article, we would like to thank Ningxia Key Laboratory of Stem Cell and Regenerative Medicine,
401 Institute of Medical Sciences and Laboratory Animal Center of Ningxia Medical University for providing
402 the platform and technical support.

403

404

405 Abbreviation

406 ASC apoptosis-associated speck-like protein

407 BBB Basso-Beattie-Bresnahan
408 BDNF brain-derived neurotrophic factor
409 DAMP damage-related molecular patterns
410 DHA Docosahexaenoic Acid
411 GDNF glia-derived neurotrophic factor
412 GSDMD gasdermin D
413 LBP Lycium barbarum polysaccharide
414 LbGp Lycium barbarum glucopeptide
415 NLRP3 NOD-like receptor protein-3
416 NADPH nicotinamide adenine dinucleotide phosphate oxidase
417 ROS reactive oxygen species
418 SCI spinal cord injury

419 References

- 420 1. Li B, Qi J, Cheng P, Yin P, Hu G, Wang L, Liu Y, Liu J, Zeng X, Hu J, Zhou M: **Traumatic**
421 **spinal cord injury mortality from 2006 to 2016 in China.** *The Journal of Spinal Cord*
422 *Medicine* 2020, **44**:1005-1010.
- 423 2. Papatheodorou A, Stein A, Bank M, Sison CP, Gibbs K, Davies P, Bloom O: **High-Mobility**
424 **Group Box 1 (HMGB1) Is Elevated Systemically in Persons with Acute or Chronic**
425 **Traumatic Spinal Cord Injury.** *J Neurotrauma* 2017, **34**:746-754.
- 426 3. Woodburn SC, Bollinger JL, Wohleb ES: **The semantics of microglia activation:**
427 **neuroinflammation, homeostasis, and stress.** *J Neuroinflammation* 2021, **18**:258.
- 428 4. Hanisch UK: **Microglia as a source and target of cytokines.** *Glia* 2002, **40**:140-155.
- 429 5. Swaroop S, Mahadevan A, Shankar SK, Adlakha YK, Basu A: **HSP60 critically regulates**
430 **endogenous IL-1beta production in activated microglia by stimulating NLRP3**
431 **inflammasome pathway.** *J Neuroinflammation* 2018, **15**:177.
- 432 6. David S, Kroner A: **Repertoire of microglial and macrophage responses after spinal**
433 **cord injury.** *Nat Rev Neurosci* 2011, **12**:388-399.
- 434 7. Mortezaee K, Khanlarkhani N, Beyer C, Zendedel A: **Inflammasome: Its role in traumatic**
435 **brain and spinal cord injury.** *J Cell Physiol* 2018, **233**:5160-5169.
- 436 8. Broz P, Dixit VM: **Inflammasomes: mechanism of assembly, regulation and signalling.**
437 *Nat Rev Immunol* 2016, **16**:407-420.
- 438 9. Grace PM, Strand KA, Galer EL, Urban DJ, Wang X, Baratta MV, Fabisiak TJ, Anderson ND,
439 Cheng K, Greene LI, et al: **Morphine paradoxically prolongs neuropathic pain in rats**
440 **by amplifying spinal NLRP3 inflammasome activation.** *Proc Natl Acad Sci U S A* 2016,
441 **113**:E3441-3450.
- 442 10. Yan Y, Jiang W, Liu L, Wang X, Ding C, Tian Z, Zhou R: **Dopamine controls systemic**
443 **inflammation through inhibition of NLRP3 inflammasome.** *Cell* 2015, **160**:62-73.
- 444 11. Heneka MT, McManus RM, Latz E: **Inflammasome signalling in brain function and**
445 **neurodegenerative disease.** *Nat Rev Neurosci* 2018, **19**:610-621.
- 446 12. Rathinam VA, Vanaja SK, Fitzgerald KA: **Regulation of inflammasome signaling.** *Nat*
447 *Immunol* 2012, **13**:333-342.
- 448 13. Zhang Y, Murugesan P, Huang K, Cai H: **NADPH oxidases and oxidase crosstalk in**
449 **cardiovascular diseases: novel therapeutic targets.** *Nat Rev Cardiol* 2020, **17**:170-194.

- 450 14. Chan AH, Schroder K: **Inflammasome signaling and regulation of interleukin-1 family**
451 **cytokines.** *J Exp Med* 2020, **217**.
- 452 15. Tian Geng-Yuan WCaFY-C: **Isolation, purification and proties of LbGp and**
453 **Characterization of It's Glycan-Peptide Bond** *Acta Biochimica et Biophysica Sinica* 1995,
454 **27:200-206**.
- 455 16. Zhang L, Zhuang X, Chen Y, Xia H: **Intravenous transplantation of olfactory bulb**
456 **ensheathing cells for a spinal cord hemisection injury rat model.** *Cell Transplant* 2019,
457 **28:1585-1602**.
- 458 17. Zhao ZK, Yu HL, Liu B, Wang H, Luo Q, Ding XG: **Antioxidative mechanism of Lycium**
459 **barbarum polysaccharides promotes repair and regeneration following cavernous**
460 **nerve injury.** *Neural Regen Res* 2016, **11:1312-1321**.
- 461 18. Allen SJ, Watson JJ, Shoemark DK, Barua NU, Patel NK: **GDNF, NGF and BDNF as**
462 **therapeutic options for neurodegeneration.** *Pharmacol Ther* 2013, **138:155-175**.
- 463 19. Xing X, Liu F, Xiao J, So KF: **Neuro-protective Mechanisms of Lycium barbarum.**
464 *Neuromolecular Med* 2016, **18:253-263**.
- 465 20. Xiao J, Zhu Y, Liu Y, Tipoe GL, Xing F, So KF: **Lycium barbarum polysaccharide attenuates**
466 **alcoholic cellular injury through TXNIP-NLRP3 inflammasome pathway.** *Int J Biol*
467 *Macromol* 2014, **69:73-78**.
- 468 21. Leng F, Edison P: **Neuroinflammation and microglial activation in Alzheimer disease:**
469 **where do we go from here?** *Nat Rev Neurol* 2021, **17:157-172**.
- 470 22. Ogawa S, Hattori K, Sasayama D, Yokota Y, Matsumura R, Matsuo J, Ota M, Hori H, Teraishi
471 T, Yoshida S, et al: **Reduced cerebrospinal fluid ethanolamine concentration in major**
472 **depressive disorder.** *Sci Rep* 2015, **5:7796**.
- 473 23. Nitsch RM, Blusztajn JK, Pittas AG, Slack BE, Growdon JH, Wurtman RJ: **Evidence for a**
474 **membrane defect in Alzheimer disease brain.** *Proc Natl Acad Sci U S A* 1992, **89:1671-**
475 **1675**.
- 476 24. Gwanyanya A, Godsmark CN, Kelly-Laubscher R: **Ethanolamine: A Potential Promoiety**
477 **with Additional Effects on the Brain.** *CNS Neurol Disord Drug Targets* 2022, **21:108-**
478 **117**.
- 479 25. Yan Y, Jiang W, Spinetti T, Tardivel A, Castillo R, Bourquin C, Guarda G, Tian Z, Tschopp J,
480 Zhou R: **Omega-3 Fatty Acids Prevent Inflammation and Metabolic Disorder through**
481 **Inhibition of NLRP3 Inflammasome Activation.** *Immunity* 2013, **38:1154-1163**.
- 482 26. Niazi ZR, Silva GC, Ribeiro TP, Leon-Gonzalez AJ, Kassem M, Mirajkar A, Alvi A, Abbas M,
483 Zgheel F, Schini-Kerth VB, Auger C: **EPA:DHA 6:1 prevents angiotensin II-induced**
484 **hypertension and endothelial dysfunction in rats: role of NADPH oxidase- and COX-**
485 **derived oxidative stress.** *Hypertens Res* 2017, **40:966-975**.
- 486 27. Farooq MA, Gaertner S, Amoura L, Niazi ZR, Park SH, Qureshi AW, Oak MH, Toti F, Schini-
487 Kerth VB, Auger C: **Intake of omega-3 formulation EPA:DHA 6:1 by old rats for 2 weeks**
488 **improved endothelium-dependent relaxations and normalized the expression level**
489 **of ACE/AT1R/NADPH oxidase and the formation of ROS in the mesenteric artery.**
490 *Biochem Pharmacol* 2020, **173:113749**.
- 491 28. Liu ZH, Huang YC, Kuo CY, Chuang CC, Chen CC, Chen NY, Yip PK, Chen JP: **Co-Delivery**
492 **of Docosahexaenoic Acid and Brain-Derived Neurotropic Factor from Electrospun**
493 **Aligned Core-Shell Fibrous Membranes in Treatment of Spinal Cord Injury.**

- 494 *Pharmaceutics* 2022, **14**.
- 495 29. Cisbani G, Metherel AH, Smith ME, Bazinet RP: **Murine and human microglial cells are**
496 **relatively enriched with eicosapentaenoic acid compared to the whole brain.**
497 *Neurochem Int* 2021, **150**:105154.
- 498 30. Saini RK, Keum YS: **Omega-3 and omega-6 polyunsaturated fatty acids: Dietary**
499 **sources, metabolism, and significance - A review.** *Life Sci* 2018, **203**:255-267.
- 500 31. Fourrier C, Remus-Borel J, Greenhalgh AD, Guichardant M, Bernoud-Hubac N, Lagarde
501 M, Joffre C, Laye S: **Docosahexaenoic acid-containing choline phospholipid**
502 **modulates LPS-induced neuroinflammation in vivo and in microglia in vitro.** *J*
503 *Neuroinflammation* 2017, **14**:170.
- 504 32. Anjum A, Yazid MD, Fauzi Daud M, Idris J, Ng AMH, Selvi Naicker A, Ismail OHR, Athi
505 Kumar RK, Lokanathan Y: **Spinal Cord Injury: Pathophysiology, Multimolecular**
506 **Interactions, and Underlying Recovery Mechanisms.** *Int J Mol Sci* 2020, **21**.
- 507 33. McDonald JW, Sadowsky C: **Spinal-cord injury.** *Lancet* 2002, **359**:417-425.
- 508 34. Ahuja CS, Nori S, Tetreault L, Wilson J, Kwon B, Harrop J, Choi D, Fehlings MG: **Traumatic**
509 **Spinal Cord Injury-Repair and Regeneration.** *Neurosurgery* 2017, **80**:S9-S22.
- 510 35. Gong X, Cheng J, Zhang K, Wang Y, Li S, Luo Y: **Transcriptome sequencing reveals**
511 **Gastrodia elata Blume could increase the cell viability of eNPCs under hypoxic**
512 **condition by improving DNA damage repair ability.** *J Ethnopharmacol* 2022,
513 **282**:114646.
- 514 36. Zhang Q, Liu X, Yan L, Zhao R, An J, Liu C, Yang H: **Danshen extract (Salvia miltiorrhiza**
515 **Bunge) attenuate spinal cord injury in a rat model: A metabolomic approach for the**
516 **mechanism study.** *Phytomedicine* 2019, **62**:152966.
- 517 37. Liu M, Zhou L, Chen Z, Hu C: **Analgesic effect of iridoid glycosides from Paederia**
518 **scandens (LOUR.) MERRILL (Rubiaceae) on spared nerve injury rat model of**
519 **neuropathic pain.** *Pharmacol Biochem Behav* 2012, **102**:465-470.
- 520 38. Xian M, Cai J, Zheng K, Liu Q, Liu Y, Lin H, Liang S, Wang S: **Aloe-emodin prevents nerve**
521 **injury and neuroinflammation caused by ischemic stroke via the PI3K/AKT/mTOR**
522 **and NF-kappaB pathway.** *Food Funct* 2021, **12**:8056-8067.
- 523 39. Lam CS, Tipoe GL, So KF, Fung ML: **Neuroprotective mechanism of Lycium barbarum**
524 **polysaccharides against hippocampal-dependent spatial memory deficits in a rat**
525 **model of obstructive sleep apnea.** *PLoS One* 2015, **10**:e0117990.
- 526 40. Chen YS, Lian YZ, Chen WC, Chang CC, Tinkov AA, Skalny AV, Chao JC: **Lycium barbarum**
527 **Polysaccharides and Capsaicin Inhibit Oxidative Stress, Inflammatory Responses, and**
528 **Pain Signaling in Rats with Dextran Sulfate Sodium-Induced Colitis.** *Int J Mol Sci* 2022,
529 **23**.
- 530 41. Al Mamun A, Wu Y, Monalisa I, Jia C, Zhou K, Munir F, Xiao J: **Role of pyroptosis in spinal**
531 **cord injury and its therapeutic implications.** *J Adv Res* 2021, **28**:97-109.
- 532 42. Baazm M, Behrens V, Beyer C, Nikoubashman O, Zendedel A: **Regulation of**
533 **Inflammasomes by Application of Omega-3 Polyunsaturated Fatty Acids in a Spinal**
534 **Cord Injury Model.** *Cells* 2021, **10**.
- 535 43. Lacombe RJS, Chouinard-Watkins R, Bazinet RP: **Brain docosahexaenoic acid uptake**
536 **and metabolism.** *Mol Aspects Med* 2018, **64**:109-134.
- 537 44. Lalancette-Hebert M, Julien C, Cordeau P, Bohacek I, Weng YC, Calon F, Kriz J:

- 538 **Accumulation of dietary docosahexaenoic acid in the brain attenuates acute immune**
539 **response and development of postischemic neuronal damage.** *Stroke* 2011, **42**:2903-
540 2909.
- 541 45. Almeida RD, Manadas BJ, Melo CV, Gomes JR, Mendes CS, Graos MM, Carvalho RF,
542 Carvalho AP, Duarte CB: **Neuroprotection by BDNF against glutamate-induced**
543 **apoptotic cell death is mediated by ERK and PI3-kinase pathways.** *Cell Death Differ*
544 2005, **12**:1329-1343.
- 545 46. Chao MV, Rajagopal R, Lee FS: **Neurotrophin signalling in health and disease.** *Clin Sci*
546 (*Lond*) 2006, **110**:167-173.
- 547 47. Marosi K, Mattson MP: **BDNF mediates adaptive brain and body responses to**
548 **energetic challenges.** *Trends Endocrinol Metab* 2014, **25**:89-98.
- 549 48. Yang JL, Lin YT, Chuang PC, Bohr VA, Mattson MP: **BDNF and exercise enhance neuronal**
550 **DNA repair by stimulating CREB-mediated production of apurinic/aprimidinic**
551 **endonuclease 1.** *Neuromolecular Med* 2014, **16**:161-174.
- 552 49. Peng Z, Zhang C, Yan L, Zhang Y, Yang Z, Wang J, Song C: **EPA is More Effective than**
553 **DHA to Improve Depression-Like Behavior, Glia Cell Dysfunction and Hippocampal**
554 **Apoptosis Signaling in a Chronic Stress-Induced Rat Model of Depression.** *Int J Mol*
555 *Sci* 2020, **21**.
- 556
557
558

Figures

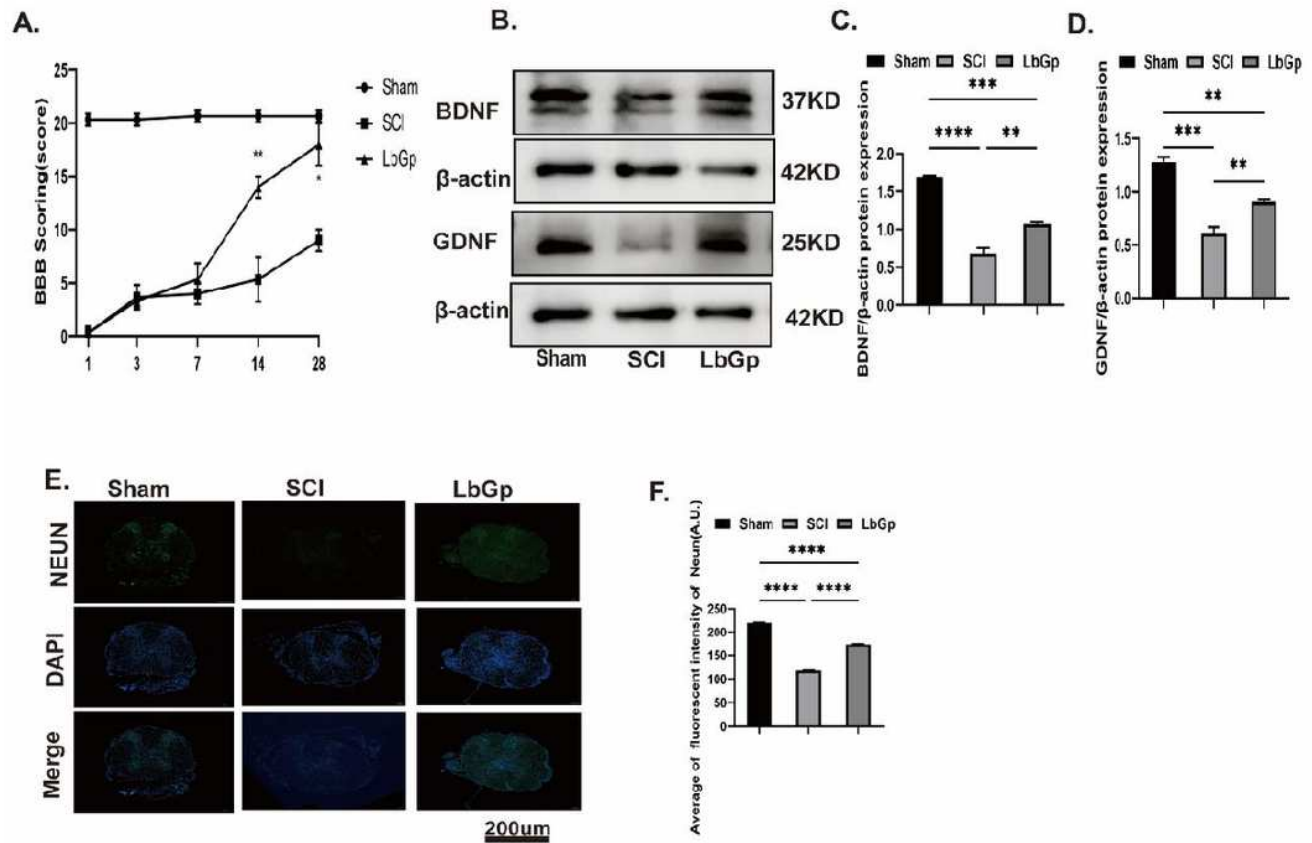


Figure 1

Lycium Barbarum Glycopeptide promote nerve regeneration and benefit motor function recovery. (A) Motor function was evaluated using the BBB score in each group, the LbGp treatment group had higher score than the SCI group since the second week and was not statistically different from the sham group. (n=3 for each group) *p 0.05, SCI VS LbGp treatment group. (B-D) detected the expression level of BDNF and GDNF in spinal cord tissue by western blotting. (E-F) Fluorescence staining micrographs of NEUN protein in spinal cord tissues of different groups. Data represent the means SEM of at least 3 independent experiments, Scale bar 200um. n=3 per group, *p 0.05, **p 0.01, ***p 0.001, ****p 0.0001 versus each group.

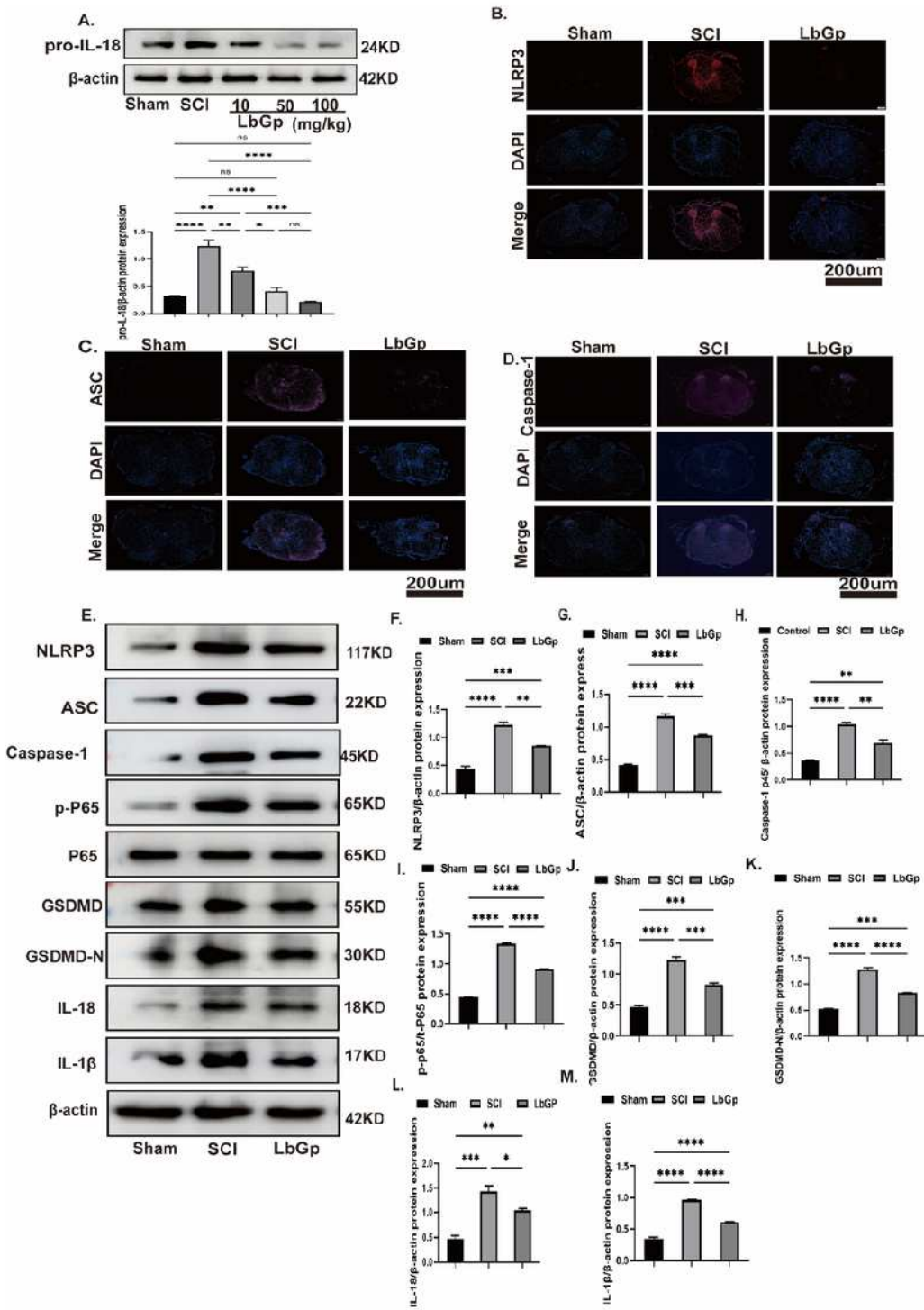


Figure 2

Lycium Barbarum Glycopeptide inhibit NF- κ B and pyroptosis-related proteins in vivo

(A) Spinal cord injury treatment with different doses (10mg/kg-100mg/kg) of LbGp reduces pro-IL-18 protein expression levels. (B-C) Fluorescence staining micrographs of NLRP3, ASC, Caspase-1 protein 7th days in spinal cord tissues of different groups. (E-M) On day 7, the expression level of each group of

NLRP3, ASC, Caspase-1, p-P65, P-65, GSDMD, GSDMD-N, IL-18, IL-1 β protein in spinal cord tissue was detected by western blotting. Data represent the means SEM of at least 3 independent experiments

Scale bar 200um, n=3 per group, *p 0.05, **p 0.01, ***p 0.001, ****p 0.0001, versus each group.

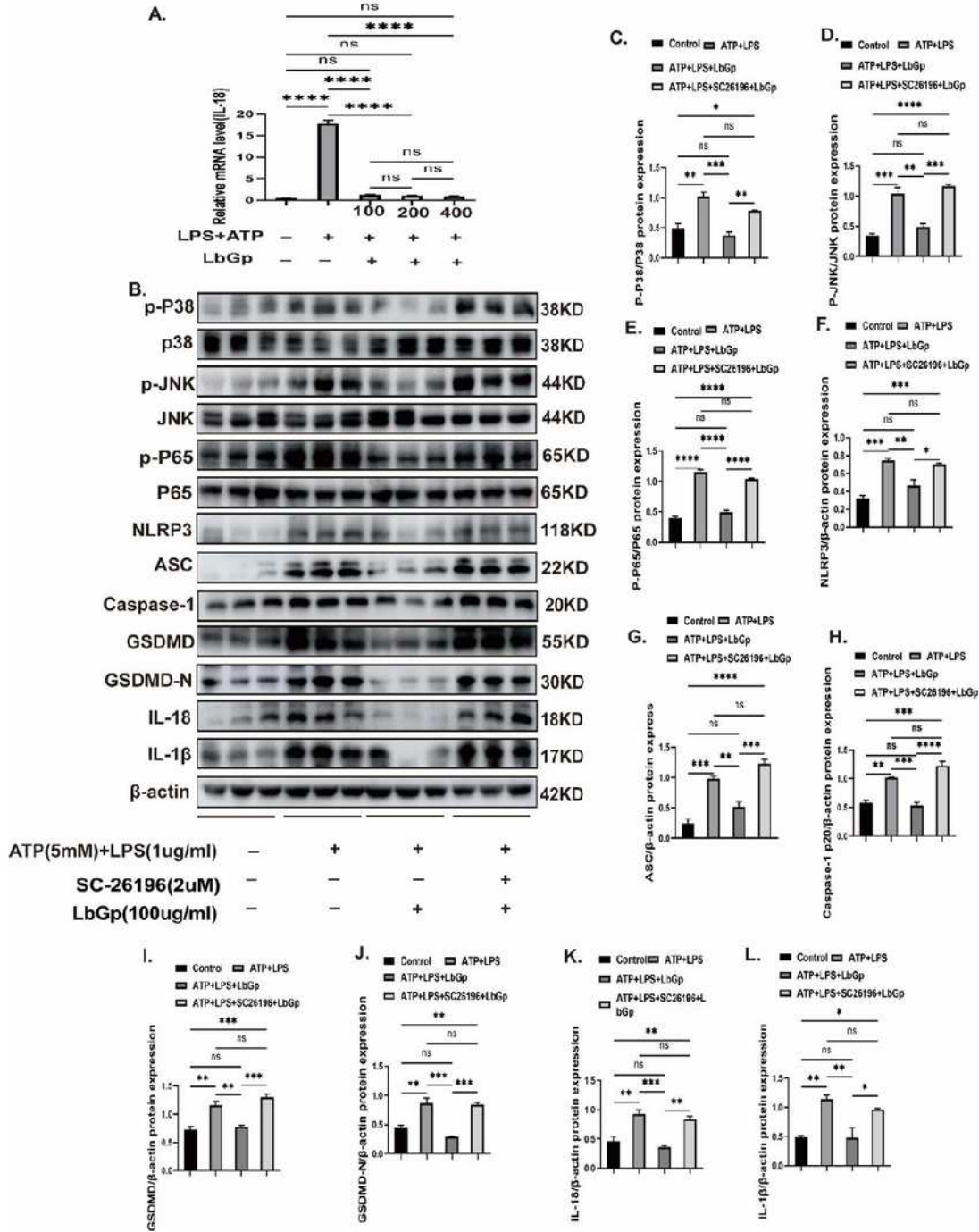


Figure 3

Lycium Barbarum Glycopeptide inhibited microglia MAPKs/NF- κ B and pyroptosis-related pathways. (A) mRNA expression level of IL-18 in ATP+LPS stimulated Microglia treatment with different doses(100ug/kg-400ug/ml) of LbGp. (B-L) The expression levels of p-P38,P38,p-JNK,JNK, p-P65, P-65, NLRP3, Caspase-1-p20, ASC, GSDMD, GSDMD-N , IL-18, IL-1 β protein in each group after microglia were activated in western blotting experiments. Data represent the means SEM of at least 3 independent experiments *p 0.05, **p 0.01, ***p 0.001, ****p 0.0001 versus each group.

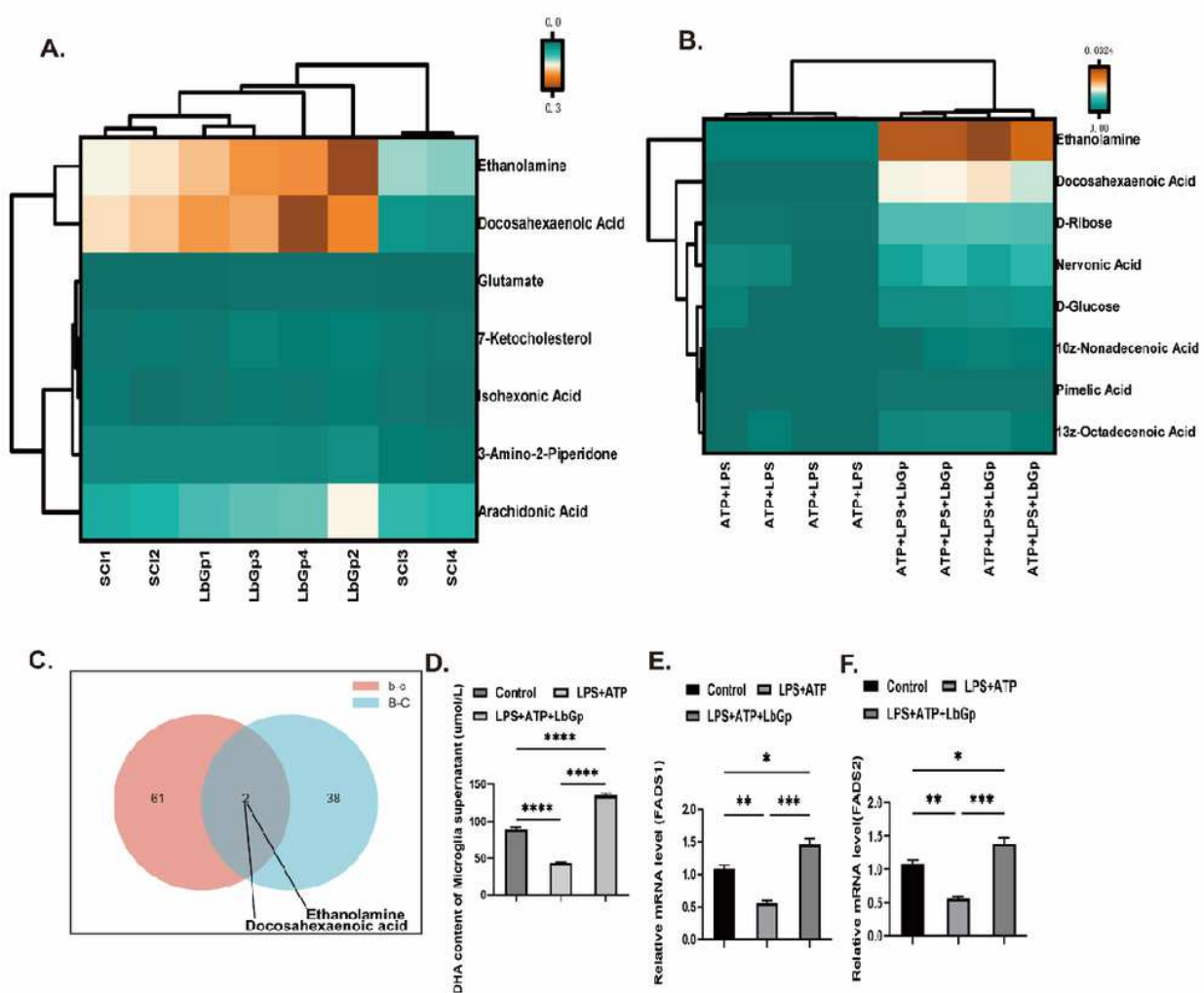


Figure 4

Lycium Barbarum Glycopeptide Induces microglia to secrete DHA

(A) Heat map of differential metabolic substances between the SCI and LbGp groups in spinal cord tissue. (B) Heat map of differential metabolic substances between ATP+LPS and LbGp treatment groups in

microglia supernatants. (C) Venn diagram of elevated metabolites in spinal cord tissues LbGp-treated group and microglia LbGp-treated group. (D) After ATP+LPS activation of microglia for 4h, LbGp was given to incubate for 24h, cell supernatants were assayed for DHA. (E-F) mRNA expression level of FADs1 and FADs2 in ATP+LPS stimulated Microglia treatment with LbGp. Data represent the means \pm SEM of at least 3 independent experiments n=6 per group, *p<0.05, **p<0.01, ***p<0.001, ****p<0.0001 versus each group.

Figure.

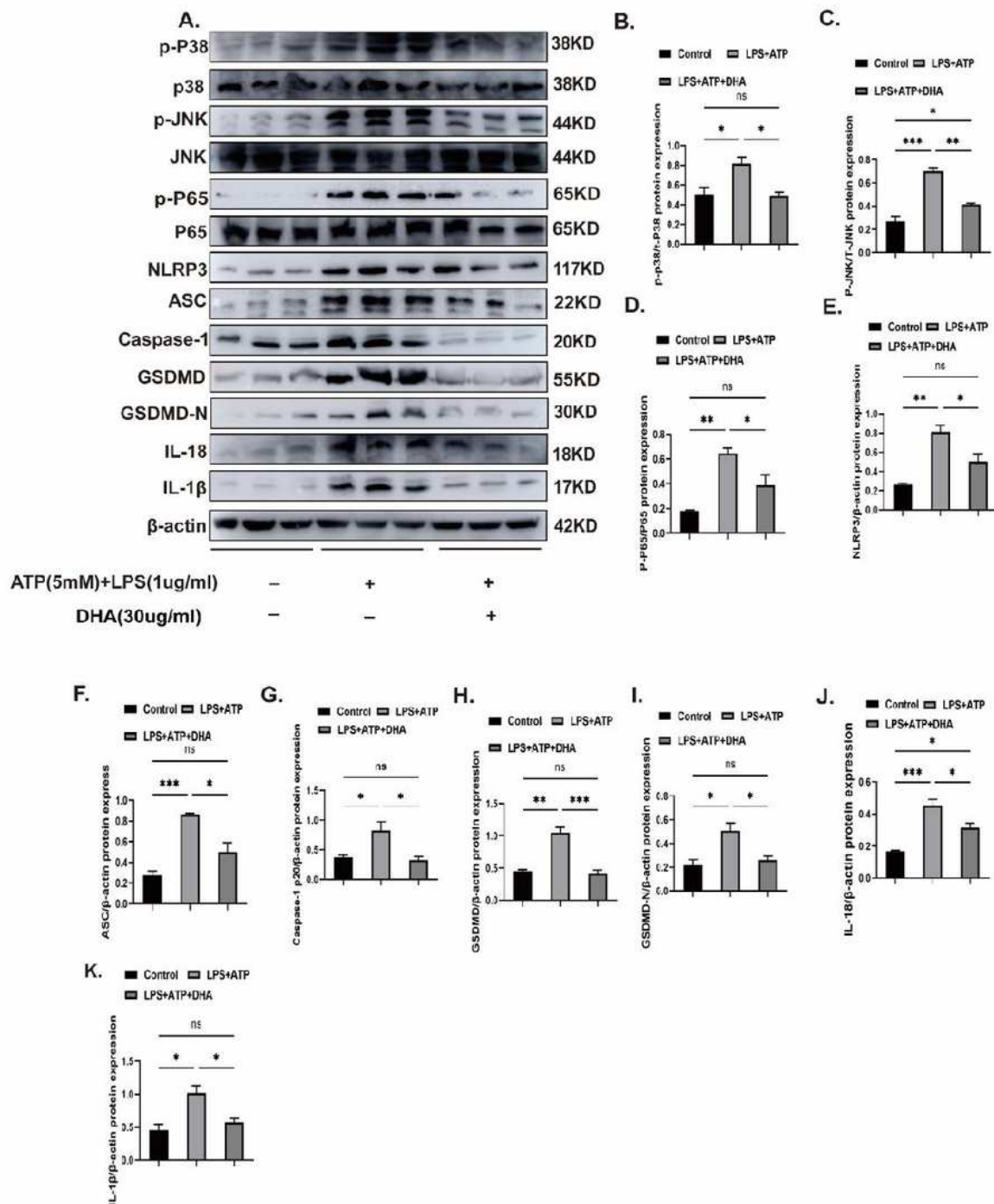


Figure 5

DHA inhibited microglia MAPKs/NF- κ B and pyroptosis-related pathways. (A-K) The expression levels of p-P38, P38, p-JNK, JNK, p-P65, P-65, NLRP3, Caspase-1-p20, ASC, GSDMD, GSDMD-N, IL-18, IL-1 β protein in each group after microglia were activated in western blotting experiments. Data represent the means SEM of at least 3 independent experiments *p 0.05, **p 0.01, ***p 0.001, ****p 0.0001 versus each group.

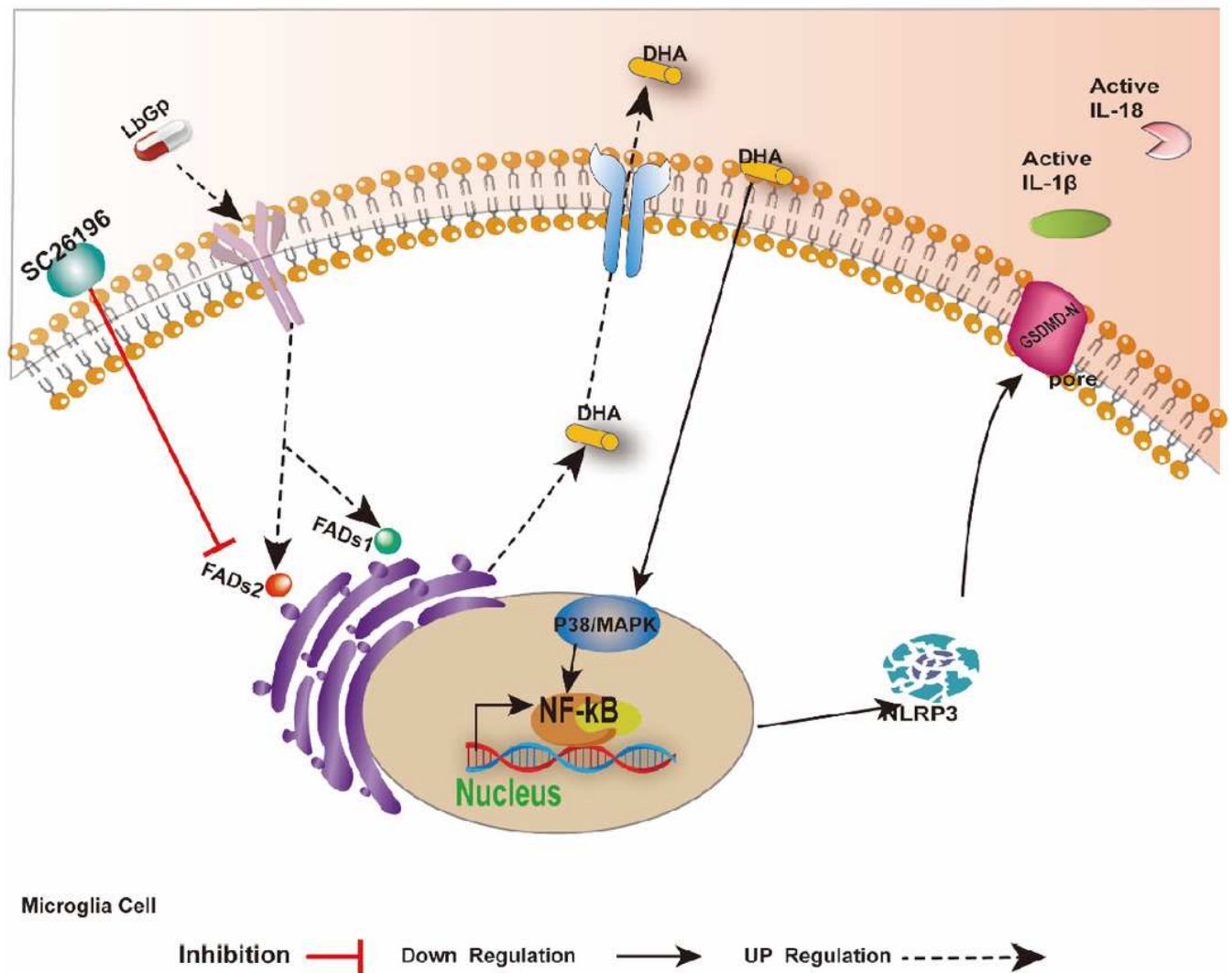


Figure 6

A model illustrating the role of LbGp in alleviating the inflammatory microenvironment by prompting microglia to secrete DHA to inhibit the MAPKs/NF-kB and pyroptosis pathway.

LbGP action on microglia promotes high expression of FADs1 and FADs2, key enzymes for GD synthesis on the endoplasmic reticulum, prompting microglia to secrete DHA, which further and improves the inflammatory microenvironment via inhibits MAPKs/NF-kB and pyroptosis pathway. However, the intervention of the FADs2 inhibitor SC-26196 diminishes the inhibitory effect of LbGP on neuroinflammation.

Supplementary Files

This is a list of supplementary files associated with this preprint. Click to download.

- [Supplementmaterial.pdf](#)
- [Table.docx](#)